

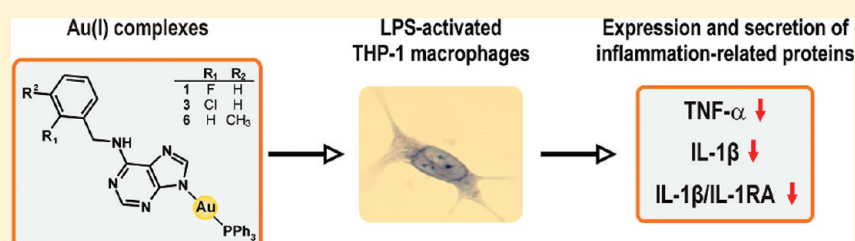
Anti-inflammatory Active Gold(I) Complexes Involving 6-Substituted-Purine Derivatives

Zdeněk Trávníček,^{*,†} Pavel Štarha,[†] Ján Vančo,[†] Tomáš Šilha,[†] Jan Hošek,^{†,‡} Pavel Suchý, Jr.,[§] and Gabriela Pražanová[§]

[†]Regional Centre of Advanced Technologies and Materials, Department of Inorganic Chemistry, Faculty of Science, Palacký University, 17 listopadu 1192/12, 771 46 Olomouc, Czech Republic

[‡]Department of Natural Drugs, and [§]Department of Human Pharmacology and Toxicology, Faculty of Pharmacy, University of Veterinary and Pharmaceutical Sciences Brno, Palackého 1/3, 612 42 Brno, Czech Republic

S Supporting Information



ABSTRACT: The gold(I) complexes of the general formula $[\text{Au}(\text{L}_n)(\text{PPh}_3)] \cdot x\text{H}_2\text{O}$ (1–8; $n = 1–8$ and $x = 0–1.5$), where L_n stands for a deprotonated form of the benzyl-substituted derivatives of 6-benzylaminopurine, were prepared, thoroughly characterized (elemental analyses, FT-IR, Raman and multinuclear NMR spectroscopy, ESI+ mass spectrometry, conductivity, DFT calculations), and studied for their *in vitro* cytotoxicity and *in vitro* and *in vivo* anti-inflammatory effects on LPS-activated macrophages (derived from THP-1 cell line) and using the carrageenan-induced hind paw edema model on rats. The obtained results indicate that the representative complexes (1, 3, 6) exhibit a strong ability to reduce the production of pro-inflammatory cytokines $\text{TNF-}\alpha$, $\text{IL-1}\beta$ and HMGB1 without influence on the secretion of anti-inflammatory cytokine IL-1RA in the LPS-activated macrophages. The complexes also significantly influence the formation of edema, caused by the intraplantar application of polysaccharide λ -carrageenan to rats *in vivo*. All the tested complexes showed similar or better biological effects as compared with Auranofin, but contrary to Auranofin they were found to be less cytotoxic *in vitro*. The obtained results clearly indicate that the gold(I) complexes behave as very effective anti-inflammatory agents and could prove to be useful for the treatment of difficult to treat inflammatory diseases such as rheumatoid arthritis.

INTRODUCTION

Adenine derivatives substituted at the N6 position, such as 6-benzylaminopurine (Bap) and its benzyl-substituted analogues, belong to the group of both natural and artificial growth regulators called cytokinins.¹ Furthermore, the Bap derivatives substituted besides the benzyl aromatic ring also at a purine moiety may be integrated into a family of cyclin dependent kinase inhibitors, such as 2-[(R)-(1-ethyl-2-hydroxyethylamino)]-6-benzylamino-9-isopropylpurine (R-roscovitine),² which have received attention because of their biological, particularly antitumor, activity.³ From the coordination or bioinorganic chemistry point of view, variously substituted Bap derivatives represent a group of polydentate N-donor ligands biologically active themselves, and moreover, the transition metal complexes involving such ligands were found to be highly biologically active as well.^{4–7}

Gold(I) coordination compounds are known to play several biochemical roles.^{8–10} Focusing on the gold(I) triphenylphosphine (PPh_3) complexes involving N-donor heterocyclic ligands, some compounds of the general composition $[\text{Au}(\text{L})-$

$(\text{PPh}_3)]$ were tested and found to be *in vitro* antimicrobial active agents [HL = 4-amino-N-(5-methylisoxazole-3-yl)-benzenesulfonamide, mercaptopropionic acid, mercaptoglucosaminic acid and mercaptobenzoic acid, D-penicillamine, pyrazole, imidazole, 1,2,3-triazole, 1,2,4-triazole, tetrazole].^{11–13} *In vitro* antitumor activity against the cervical carcinoma (HeLa-229), ovarian carcinoma (A2780), and cisplatin-resistant ovarian carcinoma (A2780cis) human cancer cell lines was investigated for 10 gold(I) complexes of the above-mentioned general composition with the anions of 3-(aryl)-2-sulfanypropionic acid.¹⁴ Recently, it has been reported that Auranofin [triethylphosphine-(2,3,4,6-tetra-O-acetyl- β -D-thiopyranosato)-gold(I)] and other gold(I) and gold(III) complexes have a positive therapeutic effect on HIV-infection^{15,16} and their application could be beneficial for AIDS suffering patients.¹⁷

Nevertheless, the best known application of gold(I) compounds concerns the treatment of rheumatoid arthritis.

Received: October 20, 2011

Published: April 30, 2012

Nowadays, their representatives Auranofin, Solganal [$\{(2S,3R,4S,5S,6R)-3,4,5\text{-trihydroxy-6-(hydroxymethyl)-oxane-2-thiolato}\}\text{gold(I)}$], and Myochrysin [sodium ((2-carboxy-1-carboxylatoethyl)thiolato)gold(I), GST] are the most important clinically used gold(I) complexes.^{18,19} An administration of metallic gold or its complexes for the treatment of different diseases, known as chrysotherapy, came through various phases during its several thousand years history. The last one started in 1929,²⁰ when the first parenteral drug preparations, containing gold or its compounds, were introduced into the therapy of inflammation-related indications. A significant progress in chrysotherapy occurred in mid-1980s, when the first oral formulations, containing drug Auranofin,²¹ were approved. At the time of the introduction of parenteral chrysotherapy, only a little was known about the pharmacodynamics and mechanism of action of gold-containing compounds in biological systems. Since then, major advances have been achieved to elucidate the mechanisms of action, although this topic is not completely closed even nowadays.^{16,22–25} Several mechanisms of action were proposed to explain the anti-inflammatory activity of gold-containing drugs. A lot of discussions were dedicated to the identification of the biologically active end-products of gold drugs metabolism, and most of investigators agreed that Au(I)²⁶ as well as Au(I) metabolites (such as $[\text{Au}(\text{CN})_2]^-$,^{27,28} Au(III),²⁹ or Au nanoparticles^{30,31}) play a major role. Because of the composition and structure diversities of active species, a number of various mechanisms of action were proposed. Specifically: (a) the mechanism induced by Au(I) compounds and based on the cellular enzymes inhibition,³² especially the serine esterases, such as elastase, cathepsin G, B, K, S.^{33,34} The next identified cellular processes, also directly influenced by Au(I) compounds, may be as follows: the inhibition of lysosome enzymes release (i.e., β -glucuronidase, lysosyme) in polymorphonuclears,^{32,35} the inhibition of T-lymphocytes, macrophages, immunoglobulin levels, rheumatoid factor titers, tumor necrosis factor,³⁵ monocyte capacity to produce superoxide anions,^{36,37} bone resorption, and vascular cell adhesion molecules on endothelial cells, the release of stress proteins from macrophages and surface adhesion of polymorphonuclear neutrophils,^{38,39} the inhibition of selenium enzymes, especially activity of thioredoxin reductase,^{40,41} and expression of different oxidative-stress proteins such as ezrin or peroxiredoxins;⁴² (b) the conversion of Au(I) compounds to the $[\text{Au}(\text{CN})_2]^-$ species, which suppress oxidant production of inflammatory cells, including neutrophils, monocytes, and lymphocytes;²⁸ (c) the oxidation of Au(I) to Au(III) involved into a reversible redox process, in which Au(III) can be considered to be a better oxidant than Au(I) and dominates both the anti-inflammatory and toxic effects of gold salts;²⁹ (d) the reduction of Au(I) or Au(III) to colloidal gold Au(0),⁴³ which, similarly to Au(I), suppresses the activity of inflammatory-associated cytokines, tumor necrosis factor, immune complexes, and rheumatoid factors.⁴⁴

On the basis of the clinical success of the last-mentioned gold(I) complexes, we decided to prepare, characterize, and study anti-inflammatory activity of the prepared complexes on in vitro and in vivo models. The ability to regulate the levels of inflammatory-related cytokines TNF- α (tumor necrosis factor- α), IL-1 β (interleukin-1 β), and HMGB1 (high-mobility group protein B1), i.e., pro-inflammatory cytokines, and IL-10 (interleukin-10) and IL-1RA (interleukin-1 receptor antagonist), i.e., anti-inflammatory cytokines, were determined in vitro on lipopolysaccharide-(LPS)-stimulated macrophages derived

from the human acute monocytic leukemia (THP-1) cell line. The influence of the tested compounds on carrageenan-induced paw edema on rats was also evaluated. The obtained results are discussed within the framework of the following text.

CHEMISTRY

Synthesis and General Properties. The gold(I) complexes of the composition $[\text{Au}(\text{L}_n)(\text{PPh}_3)] \cdot \text{H}_2\text{O}$ (**1**), $[\text{Au}(\text{L}_2)(\text{PPh}_3)]$ (**2**), $[\text{Au}(\text{L}_3)(\text{PPh}_3)]$ (**3**), $[\text{Au}(\text{L}_4)(\text{PPh}_3)]$ (**4**), $[\text{Au}(\text{L}_5)(\text{PPh}_3)] \cdot 1.5\text{H}_2\text{O}$ (**5**), $[\text{Au}(\text{L}_6)(\text{PPh}_3)]$ (**6**), $[\text{Au}(\text{L}_7)(\text{PPh}_3)]$ (**7**), $[\text{Au}(\text{L}_8)(\text{PPh}_3)]$ (**8**) (Figure 1), where L_n stands

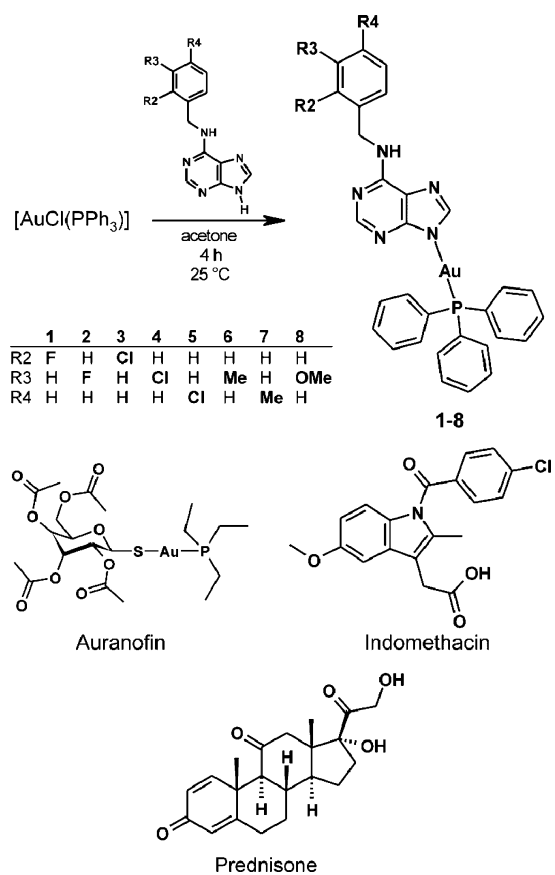


Figure 1. Synthetic pathway for the preparation of the gold(I) complexes (**1–8**) and schematic representations of Auranofin, indomethacin, and prednisone.

for the deprotonated form of the appropriate 6-benzylamino-purine derivative (see Supporting Information, Scheme S1), were prepared by the reaction of $[\text{AuCl}(\text{PPh}_3)]$ and HL_n in acetone, as described in the Experimental Section, and obtained as white powder products (see Supporting Information). Complexes **1–8** are very well soluble in *N,N'*-dimethylformamide (DMF), methanol, ethanol, and butanol and partially soluble in water at room temperature. The complexes behave as nonelectrolytes in the 10^{-3} M methanolic solutions. The presence of the water molecules of crystallization in **1** and **5** was proved by simultaneous thermogravimetric (TG) and differential thermal (DTA) analyses, which also showed the dehydrated complexes **1** and **5**, as well as the remaining gold(I) complexes, to be thermally stable up to 144–190 °C, when their thermal decay started (see Supporting Information, Figure S1). Electrospray ionization mass spectrometry in a positive mode (ESI+) mass spectra of **1–8** contain the $[\text{Au}(\text{L}_n)(\text{PPh}_3)]$

+ H]⁺ molecular peaks (in the case of the hydrated complexes **1** and **5** without the water molecules of crystallization) as well as the [HL_n + H]⁺ fragments corresponding to the respective 6-benzylaminopurine derivative. The peaks of the [Au(L_n)(PPh₃) + Na]⁺ adducts were observed in the mass spectra of **3–5** (Supporting Information, Figure S2).

NMR, IR and Raman Spectroscopy. All the hydrogen and carbon atoms of the free HL_n and PPh₃ molecules were located in the ¹H and ¹³C NMR spectra of **1–8**, except for the N6H proton, which was detected in the case of **6–8** only, and the N9H one, which was not found, due to deprotonization of HL_n in any proton spectrum of **1–8** (see Supporting Information). The highest coordination shifts ($\Delta\delta = \delta_{\text{complex}} - \delta_{\text{ligand}}$; ppm) of the signals of the 6-benzylaminopurine derivatives were calculated for the C4 and C8 atoms, which were shifted by 4.83–10.27 ppm upfield and 8.33–9.08 ppm downfield, respectively, and C8H protons shifted by 0.17–0.32 ppm upfield (see Supporting Information, Table S1). The complex **1** was also studied by ³¹P NMR showing the P-atom signal shifted by 36 ppm upfield as compared with free PPh₃. These results indicate that the 6-benzylaminopurine derivatives coordinate through the N9 atoms and PPh₃ molecule coordinates to the central gold(I) atom through the phosphorus atom. The anticipated N9-coordination of the purine moiety to the Au(I) atom within the structure of **1–8** was reported for several gold(I) complexes, such as [Au(ade)PPh₃]⁴⁵ and [Au(ade)-PEt₃]⁴⁶ where the deprotonated form of adenine (ade) coordinates to the central atom via the N9 atom of the purine moiety, as determined by the X-ray crystallographic study.

The IR and Raman spectra of **1–8** contain the $\nu(\text{C}=\text{N})_{\text{ar}}$ vibration of the purine ring of very strong intensity, whose maximum were detected at 1610–1619 cm⁻¹ (IR) and 1612–1617 cm⁻¹ (Raman) and shifted by 3–30 cm⁻¹ as compared with those observed in free 6-benzylaminopurine derivatives. The $\nu(\text{C}=\text{C})_{\text{ar}}$, $\nu(\text{C}-\text{H})_{\text{al}}$, $\nu(\text{C}-\text{H})_{\text{ar}}$ and $\nu(\text{N}-\text{H})$ vibrations were, as well as $\nu(\text{C}_{\text{ar}}-\text{Cl})$, $\nu(\text{C}_{\text{ar}}-\text{F})$, and $\nu(\text{C}_{\text{met}}-\text{H})$ of the appropriate substituent, also detected in the spectra of the complexes (see Supporting Information). The maxima assignable to $\nu(\text{Au}-\text{N})$ were detected at 543–547 cm⁻¹ (IR) and 542–593 cm⁻¹ (Raman), while the $\nu(\text{Au}-\text{P})$ stretching vibrations were observed at 338–361 cm⁻¹ (IR) and 358–368 cm⁻¹ (Raman).

Quantum Chemical Calculations. In an effort to predict the molecular structure of **1**, the knowledge based on the results of spectroscopic and other analyses were summarized, together with the known structures of similar complexes, and the built model was optimized at the DFT-level using the hybrid B3LYP functional with the LACVP+** basis set using the Spartan (version 1.1.0) software.^{47–49} Optimized geometry of the complex **1** is shown in Supporting Information, Figure S3. The gold(I) atom is bidentate-coordinated by one N9-coordinated 6-(2-fluorobenzylamino)purine anion (Au–N9 = 2.035 Å) and by one P-coordinated triphenylphosphine molecule (Au–P = 2.382 Å). More detailed discussion regarding interatomic parameters is given in Supporting Information.

■ IN VITRO ANTI-INFLAMMATORY ACTIVITY TESTING

Cytotoxicity against THP-1 Cells. The cytotoxic effect of the selected representatives of the gold(I) complexes **1**, **3**, and **6** and Auranofin was evaluated against THP-1 cells before the testing of anti-inflammatory activity itself. Complexes **1**, **3**, and **6** showed strong cytotoxic action (Figure 2) with the LD₅₀

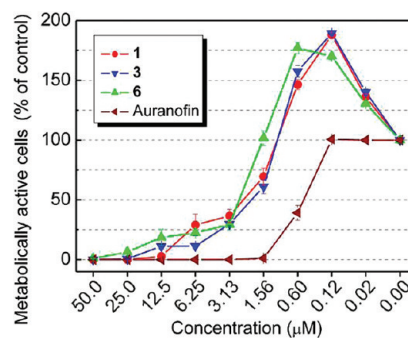


Figure 2. THP-1 cells were treated with the decreasing concentration (50.00–0.00 μM) of **1**, **3**, **6**, and Auranofin. After 24 h incubation, the number of metabolically active cells was determined by the WST-1 test. The viability was calculated as the percentage of vehicle-treated cells. The results are expressed as means ± SE for three independent experiments.

values of 1.91 μM for **1**, 1.87 μM for **3**, and 2.44 μM for **6**. On the other hand, in the range of the concentrations between 1.00 and 0.02 μM, complexes **1**, **3**, and **6** caused significant accrual of numbers of metabolically active cells, which was manifested by higher amount of formazan, formed by the NAD(P)H-oxidase enzymatic system of viable cells from the WST-1 dye. It is widely known that kinetin (6-furfurylaminopurine) itself as well as some other cytokinins (including Bap and its derivatives) are able to positively affect the cell proliferation and metabolism, and may serve as antiaging agents (for more information, see recent review, Barciszewski et al., ref. 50). It has been found that the Bap derivatives, which serve as N-donor ligands in compounds **1**, **3**, and **6**, did not influence the number of metabolically active cells in the concentrations between 3.13 and 0.02 μM (data not shown). Therefore, the observed proliferative effect is undoubtedly caused by the individual Au(I) complexes.

Cytokine Expression. The progression of inflammation is connected with the expression of many genes, which trigger, maintain, and terminate it. The cooperation of individual types of immune cells during the inflammation is driven by the cytokines. The prepared gold(I) complexes have been supposed to exhibit an anti-inflammatory effect primarily because of their similarity to Auranofin, which was demonstrated by their ability to modulate cytokine expression.⁵¹ For this purpose, the expression of inflammatory-related cytokines was determined. To better understand the activity of the complexes (**1–6**), we tested their influence on the selected pro- and anti-inflammatory cytokines in the equitoxic concentration to Auranofin, i.e., 600 nM and further also in the 100 nM concentration. The biological effect of Au complexes was compared to Auranofin (tested in the 100 nM concentration) and prednisone (tested in the 1 μM concentration).

The ability of the tested compounds to reduce gene transcription of a typical member of pro-inflammatory cytokines TNF-α is depicted in Figure 3a. The complex **1** was able to significantly decrease the level of mRNA of TNF-α at 2 and 4 h after the LPS treatment. On the other hand, all three selected complexes (**1**, **3**, and **6**) were able to reduce the TNF-α secretion by the factor of ~2.5 (see Figure 3b). This effect is more similar to the effect of prednisone than to Auranofin, which reduced the TNF-α secretion only by the factor of 1.3. The mechanism of this regulation probably lies in the post-transcriptional phase because the level of TNF-α

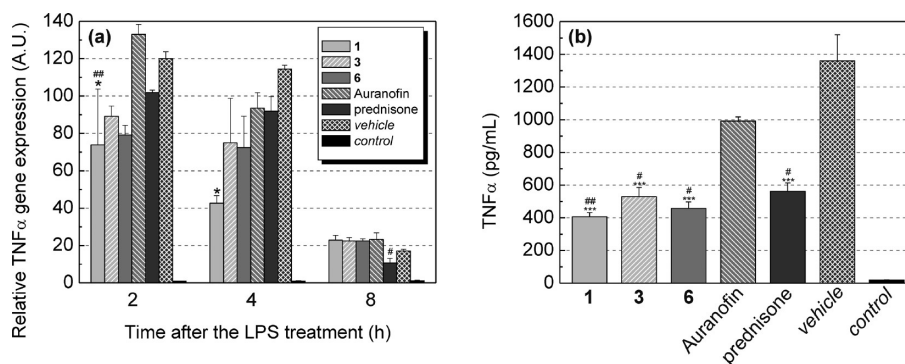


Figure 3. Effects of the gold(I) complexes and the reference drugs Auranofin and prednisone on the LPS-induced TNF- α gene expression (a) and TNF- α secretion (b). The cells were pretreated with complexes 1, 3, and 6 (600 nM) and Auranofin (100 nM), prednisone (1 μ M), or the vehicle (DMSO) only. After 1 h of incubation, the inflammatory response was induced by LPS (except for the control cells). Gene expression was measured 2, 4, and 8 h after LPS treatment, and secretion was measured 24 h after LPS adding. The results are expressed as means \pm SE for three independent experiments. AU = arbitrary unit. * Significant difference in comparison to vehicle-treated cells ($p < 0.05$), *** significant difference in comparison to vehicle-treated cells ($p < 0.001$), # significant difference in comparison to Auranofin-treated cells ($p < 0.05$), ## significant difference in comparison to Auranofin-treated cells ($p < 0.01$).

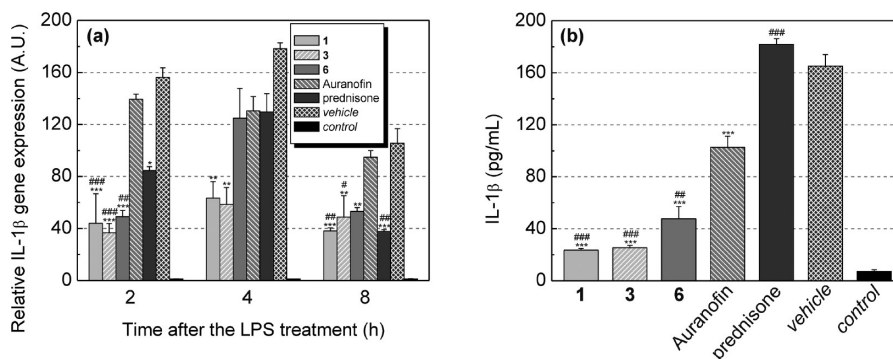


Figure 4. Effects of the gold(I) complexes and the reference drugs Auranofin and prednisone on the LPS-induced IL-1 β gene expression (a) and IL-1 β secretion (b). The cells were pretreated with complexes 1, 3, and 6 (600 nM) and Auranofin (100 nM), prednisone (1 μ M), or the vehicle (DMSO) only. After 1 h of incubation, the inflammatory response was induced by LPS (except for the control cells). Gene expression was measured 2, 4, and 8 h after LPS treatment, and secretion was measured 24 h after LPS adding. The results are expressed as means \pm SE for three independent experiments. AU = arbitrary unit. * Significant difference in comparison to vehicle-treated cells ($p < 0.05$), ** significant difference in comparison to vehicle-treated cells ($p < 0.01$), *** significant difference in comparison to vehicle-treated cells ($p < 0.001$), # significant difference in comparison to Auranofin-treated cells ($p < 0.05$), ## significant difference in comparison to Auranofin-treated cells ($p < 0.01$), ### significant difference in comparison to Auranofin-treated cells ($p < 0.001$).

mRNA was only slightly affected with the exception of 1. This correlated with the level of the secreted cytokine, where 1 showed the lowest level of the secreted TNF- α among all the tested compounds. The complexes (1, 3, and 6) were two times more efficient than Auranofin at the same effective concentration (i.e., at the same cytotoxicity levels) (Figure 3b). It has been found that the complexes (1, 3, and 6) showed the same minimal effect on the TNF- α secretion as compared to Auranofin in the equimolar concentration of 100 nM (Supporting Information, Figure S4). Auranofin was able to decrease the TNF- α secretion in concentrations higher than 5 μ M.^{51,52}

The IL-1 β pro-inflammatory cytokine was tested as the second one. Complexes 1 and 3 significantly reduced its transcription (Figure 4a). Although complex 6 also decreased the IL-1 β transcription 2 and 8 h after the LPS treatment, 4 h after adding LPS, when IL-1 β transcription reached the maximum, this compound showed only a slight effect on this action. Compound 6 exhibits very similar quantitative effect on the transcription of this gene as prednisone but slower onset of its action. These observations corresponded to the secretion of

IL-1 β (Figure 4b). The complexes 1 and 3 reduced the secreted amount of IL-1 β by the factor of ~ 7 , while complex 6 was by only 3.4. Nevertheless, it was still twice lower than for Auranofin, which decreased the amount of the secreted IL-1 β by the factor of 1.6. However, it has to be noted that Auranofin was used in the 6 times lower (equitoxic) concentration than the tested gold(I) complexes. In the 100 nM concentration, the tested Au(I) complexes showed the same or better ability to reduce the IL-1 β secretion than Auranofin. The best effect on the secretion of this cytokine was observed for complex 6, which reduced its level 5.9 times in comparison with the vehicle-treated cells, while complexes 1 and 3 decreased the IL-1 β production by the factors of 3.6 and 2, respectively (Supporting Information, Figure S5). Different behavior of complex 6 at lower concentration could be caused by a different pattern of cytotoxic curve in the range of the concentrations of 3.13 and 0.02 μ M (Figure 2). A previous study showed that Auranofin becomes more active at the concentrations over 10 μ M.⁵¹ Similar effect was observed for another Au(I)-containing drug, Myochrysine (GST). Myochrysine (GST) decreased IL-1 β secretion at the concentration of 2.6 μ M, but massive

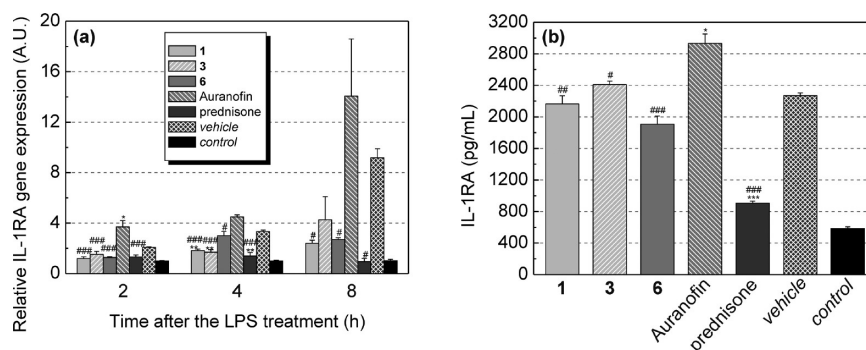


Figure 5. Effects of the gold(I) complexes and the reference drugs Auranofin and prednisone on the LPS-induced IL-1RA gene expression (a) and IL-1RA secretion (b). The cells were pretreated with complexes 1, 3, and 6 (600 nM) and Auranofin (100 nM), prednisone (1 μ M), or the vehicle (DMSO) only. After 1 h of incubation, the inflammatory response was induced by LPS (except for the control cells). Gene expression was measured 2, 4, and 8 h after LPS treatment, and secretion was measured 24 h after LPS adding. The results are expressed as means \pm SE for three independent experiments. AU = arbitrary unit. * Significant difference in comparison to vehicle-treated cells ($p < 0.05$), ** significant difference in comparison to vehicle-treated cells ($p < 0.01$), *** significant difference in comparison to vehicle-treated cells ($p < 0.001$), # significant difference in comparison to Auranofin-treated cells ($p < 0.05$), ## significant difference in comparison to Auranofin-treated cells ($p < 0.01$), ### significant difference in comparison to Auranofin-treated cells ($p < 0.001$).

decrease was achieved by the concentration of 25.6 μ M.⁵³ Interestingly, Auranofin decreased the secretion of IL-1 β without affection of its transcription, and contrariwise, prednisone reduced transcription of this cytokine but did not change its secretion.

IL-1RA acts as a physiological antagonist of IL-1 β , and their mutual balance is important for the regulation of the progress of inflammation and for maintaining the homeostasis. The tested gold(I) complexes tended to decrease its transcription, similarly to prednisone (Figure 5a). Contrary to the transcription, complexes 1, 3, and 6 did not affect the secretion of IL-1RA significantly (Figure 5b). We were not able to explain this discrepancy yet, but it is possible that these compounds decreased the transcription, and on the other side, they stabilized mRNA or positively regulated translation and secretion, and thus they preserved the physiological conditions. Prednisone decreased the level of produced IL-1RA by the factor of 2.5 (Figure 5b). The metallodrug Auranofin slightly increased IL-1RA mRNA synthesis, and this trend correlated with the IL-1RA secretion, which was 1.3 times higher than in the vehicle-treated cells. With the aim to better describe the inflammatory process in the target cells, the ratio between the expression of IL-1 β and IL-1RA was calculated. It is known that many of inflammatory diseases, like arthritis or inflammatory bowel disease, are characterized by either local overproduction of IL-1 (either IL-1 α and/or IL-1 β) and/or underproduction of IL-1RA.⁵⁴ This situation leads into absolutely or relatively higher level of pro-inflammatory cytokine IL-1. As demonstrated in Figure 6, complexes 1 and 3 reached very low IL-1 β /IL-1RA ratios, comparable to the control cells (without the LPS treatment). On the other hand, complex 6, behaved similarly to Auranofin. The steroid anti-inflammatory drug prednisone-treated cells showed this ratio almost 3 times higher than the vehicle-treated cells.

The extracellular HMGB1 also exhibits pro-inflammatory properties. As can be seen from Figure 7a, the tested compounds had only little effect on the HMGB1 transcription. However, they almost twice increased the production of mRNA for HMGB1 8 h after the LPS treatment. On the other hand, complexes 1, 3, and 6 reduced extracellular translocation of this dual-function protein, similarly to Auranofin (Figure 7b). Recently reported papers showed that the gold-containing drug

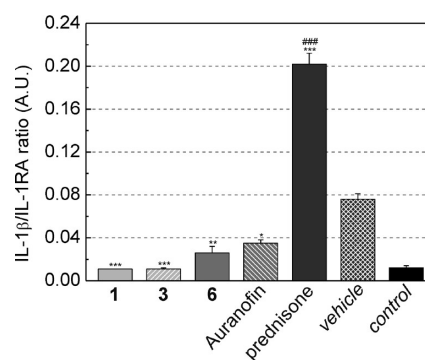


Figure 6. The calculated ratio of IL-1 β /IL-1RA. The values were obtained from the ELISA experiments of individual cytokines as it is described in Figures 4 and 5. The results are expressed as means \pm SE for three independent experiments. AU = arbitrary unit. * Significant difference in comparison to vehicle-treated cells ($p < 0.05$), ** significant difference in comparison to vehicle-treated cells ($p < 0.01$), *** significant difference in comparison to vehicle-treated cells ($p < 0.001$), ### significant difference in comparison to Auranofin-treated cells ($p < 0.001$).

Myochrysin (GST) decreased the HMGB1 secretion on different experimental models but concentrations used in these studies were higher than 50 μ M.^{55,56}

This work was also focused on the expression of anti-inflammatory cytokine IL-10. However, the THP-1 cells are not able to secrete anti-inflammatory cytokine IL-10,⁵⁷ thus only the transcription of this protein was measured. As it is shown in the Figure 8, the tested gold(I) complexes, Auranofin, and prednisone markedly reduced production of mRNA for IL-10 2 h after the LPS addition. In the other time intervals (4 and 8 h after the LPS treatment), the effect of the used compounds was minimal. The lower level of IL-10 mRNA was detected, but the study of Lampa et al.⁵⁸ described a stimulatory effect of Myochrysin (GST) on the IL-10 secretion.

The obtained results clearly showed that the transcription and expression of inflammatory-related cytokines TNF- α , IL-1 β , and HMGB1 (pro-inflammatory cytokines) and IL-10 and IL-1RA (anti-inflammatory cytokines) is influenced by the application of the tested gold(I) complexes.

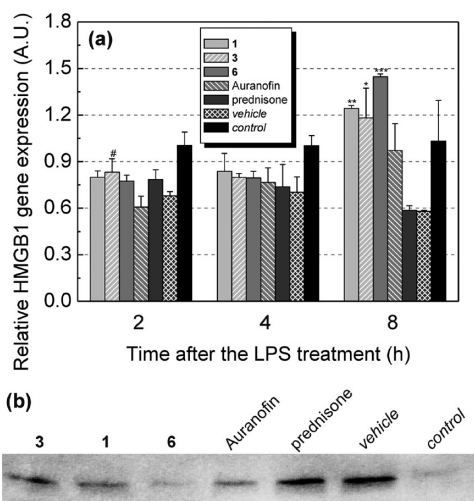


Figure 7. Effects of the gold(I) complexes and the reference drugs Auranofin and prednisone on the LPS-induced HMGB1 gene expression (a) and HMGB1 secretion (b). The cells were pretreated with complexes 1, 3, and 6 (600 nM) and Auranofin (100 nM), prednisone (1 μ M), or the vehicle (DMSO) only. After 1 h of incubation, the inflammatory response was induced by LPS (except for the control cells). Gene expression was measured 2, 4, and 8 h after LPS treatment. Secreted HMGB1 protein was detected in conditioned media by Western blot and immunodetection 24 h after LPS adding. The blot is a representative result of three independent experiments. The results of gene expression are expressed as means \pm SE for three independent experiments. AU = arbitrary unit. * Significant difference in comparison to vehicle-treated cells ($p < 0.05$), ** significant difference in comparison to vehicle-treated cells ($p < 0.01$), *** significant difference in comparison to vehicle-treated cells ($p < 0.001$), # significant difference in comparison to Auranofin-treated cells ($p < 0.05$).

Effect of the Au(I) Complexes on Carrageenan-Induced Hind Paw Edema on Rats. On the basis of in vitro experiments, the in vivo tests of anti-inflammatory activity of the complexes 1, 3, and 6 were performed using the

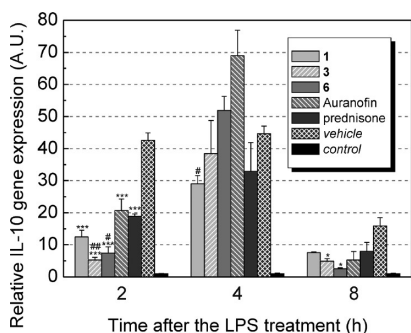


Figure 8. Effects of the gold(I) complexes and the reference drugs Auranofin and prednisone on the LPS-induced IL-10 gene expression. The cells were pretreated with complexes 1, 3, and 6 (600 nM) and Auranofin (100 nM), prednisone (1 μ M), or the vehicle (DMSO) only. After 1 h of incubation, the inflammatory response was induced by LPS (except for the control cells). The results are expressed as means \pm SE for three independent experiments. AU = arbitrary unit. * Significant difference in comparison to vehicle-treated cells ($p < 0.05$), ** significant difference in comparison to vehicle-treated cells ($p < 0.01$), *** significant difference in comparison to vehicle-treated cells ($p < 0.001$), # significant difference in comparison to Auranofin-treated cells ($p < 0.05$).

carrageenan-induced hind paw edema model, where the effect of the tested complexes on one of the symptoms of acute inflammation (i.e., the formation of edema) is investigated. Because of the structural similarity and intended purpose, we chose Auranofin as the primary standard of anti-inflammatory activity. According to the literature, it has been used in biological experiments in relatively wide range of dosage. In our experiments, we used it in the same dosages as the tested compounds, at 10 mg/kg in the form of the fine suspension in 25% DMSO (v/v in water for injections PhEur) applied intraperitoneally 30 min before the intraplantar injection of carrageenan. As a secondary standard, NSAID indomethacin was used in the dose of 5 mg/kg. The changes in the hind paw volume were continuously monitored plethysmometrically for 6 h after the carrageenan injection and assessed as percentual changes of the initial volume for every individual animal. The comprehensive overview of antiedematous activity profiles of the tested compounds are summarized in Figure 9.

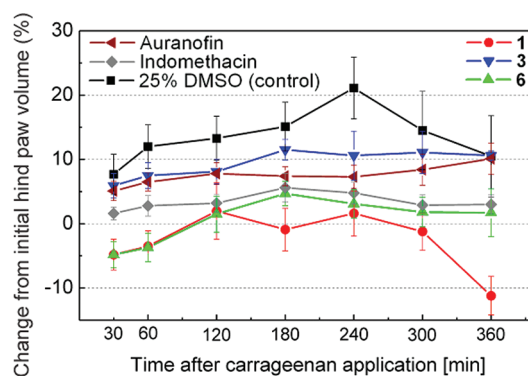


Figure 9. The time-dependent profile of antiedematous activity of the tested compounds.

The highest activity was found for 1, which was able to significantly decrease the volume of hind paw edema, even in the comparison with Auranofin ($p < 0.001$) and indomethacin ($p < 0.01$). The complex 6 was less effective than 1, and its activity profile correlated well with indomethacin, especially in the later stages of the experiment, but it showed significantly higher activity ($p < 0.001$) in comparison to Auranofin. Both complexes 1 and 6 showed antiedematous activity, comparable with the highly active derivatives of gold(I) complexes involving 3-(aryl)-2-sulfanylpropenoic acid⁵⁹ and higher activity than other gold(I) and gold(III) complexes.^{60,61} The complex 3 showed only weak activity in this experiment. This could be due to its generally lower solubility, probably related to the presence of the chloro substituent at the benzyl moiety. With the intention to better understand and describe the effect of the tested compounds on the inflammation affected tissues, the sections from the animals were evaluated by cytological and histochemical methods.

Cytological and Immunohistochemical Analyses of Animal Tissues. To assess the tissue consequences connected with the reduction of inflammation caused by the tested compounds after the intraplantar injection of carrageenan, the histopathological observations were made on the tissue sections obtained from the laboratory animals after the end of plethysmometric experiments. All animals were sacrificed by cervical dislocation, and immediately after that, the tissue samples were taken from the plantar area of hind paws.

Different histopathological changes in tissues, stained by the standard H&E-staining, were evaluated semiquantitatively using the five-point scale from 0 (no changes observed) up to 5 (maximum of changes). In addition to the classical histological investigation, the immunohistochemical detection of apoptosis (caspase 3), TNF- α , interleukin 6 (IL-6), and selectin E (CD62E) was performed. The results of the immunohistochemical IL-6 detection were due to the tissue nature being disputable because no differences were observed between the samples and control, and therefore they are not listed in the total evaluation. The results of histological and histoimmunohistochemical investigations are summarized in Table 1.

Table 1. Semiquantitative Evaluations of Different Manifestations of Inflammation in Histological and Histochemical Samples Obtained from Animals Treated with Complexes 1, 3, and 6, and the reference drugs Auranofin and indomethacin

	1	3	6	Auranofin	indomethacin	25% DMSO
Inflammation						
PNM infiltration into epidermis	0	0	0	0	0	0
infiltration PMN dermis	0	0	0	0	0	1
infiltration PMN hypodermis	2	1	2	2	2	3
total infiltration PMN	2	1	2	2	2	4
extracellular edema	1	4	1	2	2	4
intracellular edema	0	1	0	0	0	0
vasodilatation	2	2	3	1	2	3
hemorrhage	1	1	3	1	0	1
disruption score	8	10	11	8	8	16
Immunohistochemistry						
apoptosis (caspase 3)	0	0	0	0	0	0
TNF- α	1		1	3	1	4
CD 62 E	3		3	3	3	2

The inflammation infiltrate contained mainly neutrophils (polymorphonuclear cells, PMNs), vasodilatation with the hemostasis and presence of leukocytes in bloodstream, and extracellular edema. These changes provided evidence of the acute inflammation. Table 1 shows significant presence of PMNs and edematous changes in hypodermis. Total histopathological changes are qualified by the disruption score. The highest disruption scores were found in tissues exposed to 25% DMSO (Figure 10a), which was used as a vehicle for the preparation of all the tested samples, with a high amount of PMNs in hypodermis and lower in dermis. The PMN distribution was mainly diffuse in dermis in the area near the veins, and in hypodermis, a massive infiltration (more than 1000 cells in microscope field of view, 200 \times magnification) was found in thin collagen connective tissue. Immunohistochemical TNF- α detection was significantly positive, which correlates with the histological results. The selectin E (CD62E) positiveness was less conclusive due to the nature of the tissues under study. The second highest disruption score was detected in tissues exposed to 6. The inflammatory infiltrate was significantly lower, which corresponds with the TNF- α positiveness. However, significant venous dilatation (characterized by the relaxation of venous epithelium, often accompanied by venostasis) and hemorrhage significantly

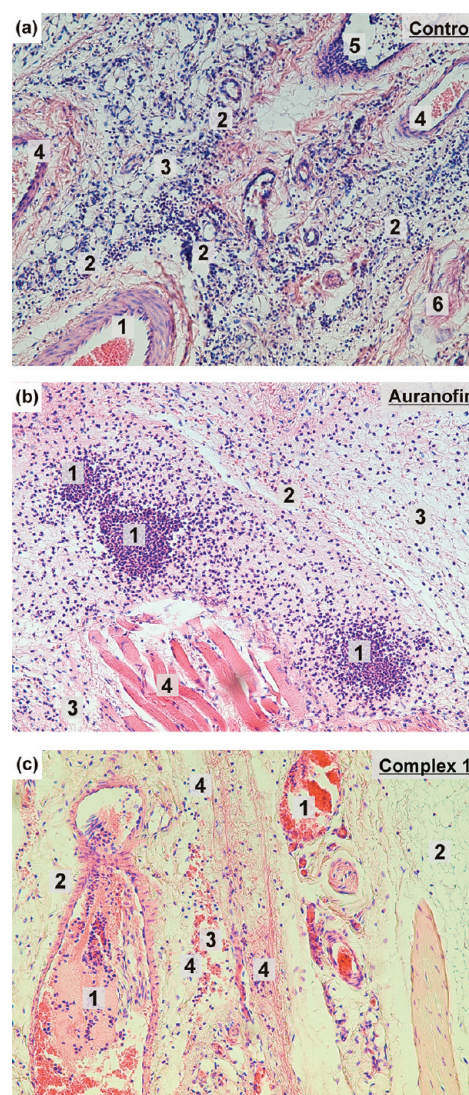


Figure 10. Histologic sections of the hind paw, stained with hematoxylin–eosin (200 \times magnification): tissue exposed to 25% DMSO (control; a) with the massive acute inflammatory reaction in the transition from dermis to hypodermis with a massive infiltrate of neutrophils (PMN); tissue exposed to Auranofin (b) and 1 (c) with the acute inflammatory reaction in the hypodermis with a slight PMN infiltrate. 1, PMN infiltrate; 2, arteriola; 3, extracellular edema; 4, dilated veins with hemostasis; 5, vein with PMN presence in the bloodstream and hemostasis; 6, collagen connective tissue; 7, slight hemorrhage characterized by the presence of erythrocytes in interstitium; 8, muscle fiber.

increased the score from the histopathological point of view. The tissue exposed to 3 can be characterized by the third highest disruption score. The inflammatory infiltrate was the lowest out of all the examined tissues; nevertheless, significant extracellular edema was present, together with a slight hydrophic degeneration of other cells (intracellular edema, characterized by small inclusions in cytoplasm of the cells). The disruption scores of the tissue exposed to Auranofin (Figure 10b), indomethacin, and 1 (Figure 10c) can be considered as identical. All the substances significantly decreased the inflammatory reaction. Apoptotic changes were not found in any of the tested samples.

Interactions of 1–3 with a Mixture of Cysteine and Glutathione by Mass Spectrometry. Because of their

properties (as soft Lewis acids), Au(I) ions prefer to form the strong coordination bonds with soft Lewis base ligands, such as thiolato or selenolato ions, or phosphine derivatives, while the latter ones form the most stable bonds. Therefore, in the biologically relevant environments (such as blood or serum), the Au(I) complexes tend to bind to sulfhydryl-containing substances, such as amino acid cysteine (Cys), or small proteins (such as glutathione, GSH) and in particular with high molecular proteins (such as albumin or globulins⁶²) with the ligand exchange mechanism. In the case of Auranofin the exchange occurs for S-ligand of tetraacetylthioglucose,⁶³ and in the next step the triethylphosphine (PEt₃) ligand is substituted by another thiolato ligand while oxidized to triethylphosphine-oxide (ref 64 and the references therein). The exchange of N-ligands for S-ligands occurs relatively quickly (within 20 min when interacting with albumin and globulins in the blood),⁶⁵ the P-ligand exchange occurs much more slowly, and it seems that in this mechanism the cooperative effects of adjacent thiolato or selenolato ligands in the neighborhood of interaction site play an important role, which is interpreted as one of the molecular mechanisms of incorporation of gold into the active site of selenium-containing flavoreductases such as thioredoxin reductase.⁶⁶

In the scope of our work, we have verified the expected behavior of complexes 1–3 (applied in the concentration of 15 μM , corresponding to the highest therapeutic blood levels of gold during chrysotherapy⁶⁷) in biologically relevant conditions⁶⁸ using a mixture of cysteine (at 290 μM concentration) and reduced glutathione (at 6 μM concentration). On the basis of the results of ESI-MS experiments, we confirmed that the complexes 1–3 react with sulfhydryl-containing substances in a concentration dependent manner so that N-ligands of 6-benzylaminopurine derivatives are substituted by cysteine, which was confirmed by the emergence of ion 580.1 m/z , corresponding to the $[\text{Cys-S-Au-PPh}_3]^+$ intermediate (see Figure 11 and Supporting Information, Figure S6). In biologically relevant concentrations of both low molecular sulfhydryl-containing compounds, the intermediate with glutathione, corresponding to $[\text{GS-Au-PPh}_3]^+$ and the mass of 766.0 m/z , reached the negligible intensity below the LOD (limit of detection, with signal-to-noise ratio $S/N < 3$).

CONCLUSIONS

The results indicated that the prepared gold(I) complexes of the type $[\text{Au}(\text{L}_n)(\text{PPh}_3)]$, involving 6-benzylaminopurine derivatives (HL_n), exhibit a strong ability to reduce the production of pro-inflammatory cytokines TNF- α , IL-1 β , and HMGB1 without influence on the secretion of anti-inflammatory cytokine IL-1RA in LPS-activated macrophages. Moreover, complexes 1 and 6 showed that they could significantly influence the formation of edema caused by the application of polysaccharide λ -carrageenan in vivo. All the tested gold(I) complexes exhibit similar or better effects as compared to Auranofin in equitoxic doses but lower cytotoxicity than Auranofin. The electrospray-ionization mass spectrometry experiments, under physiologically relevant conditions mimicking the interactions of the Au complexes with a mixture of cysteine and glutathione, confirmed that the complexes 1–3 react with sulfhydryl-containing substances in concentration-dependent manner, i.e., the 6-benzylaminopurine derivatives as ligands are substituted by cysteine, thus acting as pro-drugs, similarly to Auranofin. The obtained results entitle us to believe that the gold(I) complexes can become effective agents for

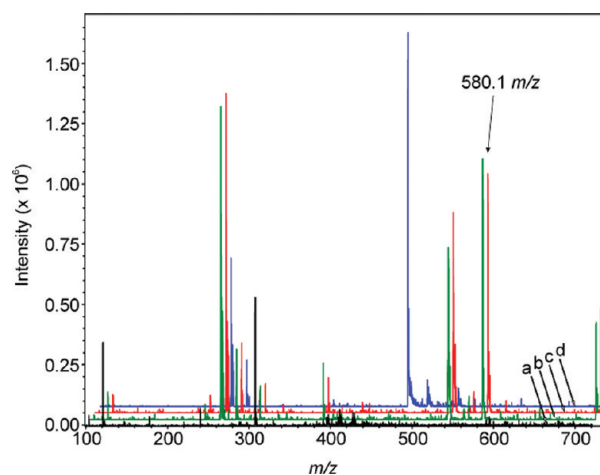


Figure 11. ESI-MS spectra of (a; black line) the mixture of physiological levels of cysteine (290 μM) and glutathione (6 μM) in 50 mM ammonium acetate in water (b; green line) the interacting system containing cysteine (290 μM) + glutathione (6 μM) + complex 3 (15 μM) in the mixture of 50 mM ammonium acetate and methanol (1:1, v/v) immediately after preparation; (c; red line) the interacting system containing cysteine (290 μM) + glutathione (6 μM) + complex 3 (15 μM) in the mixture of 50 mM ammonium acetate and methanol (1:1, v/v) 20 min after preparation, both showing the appearance of peak at 580.08 m/z , corresponding to ion $[\text{Cys-S-Au-PPh}_3]^+$; (d; blue line) complex 3 solution in methanol.

managing difficult to treat inflammatory diseases. On the basis of such promising findings, the mechanism of their action and applicability as potential drugs will be further investigated.

EXPERIMENTAL SECTION

Chemistry. Materials and General Methods. The starting materials such as AuCl₃, NaOH, and solvents were obtained from the commercial sources (Sigma–Sigma-Aldrich Co., Acros Organics Co., Lachema Co., and Fluka Co.) and used without further purification. The 6-benzylaminopurine derivatives (HL_1 – HL_8) (see Supporting Information, Scheme S1) were synthesized according to the previously published procedure.⁶⁹ The purity ($\geq 95\%$) of the final products (complexes 1–8) was confirmed by elemental analysis (CHN), with the experimental values differing less than 0.4% from the calculated ones, and by ¹H and ¹³C NMR spectroscopy.

Elemental analyses (C, H, N) were performed on a Flash 2000 CHNO-S analyzer (Thermo Scientific). Conductivity measurements of 10^{-3} M methanol solutions of the prepared complexes were carried out using a conductometer 340i/SET (WTW) at 25 °C. IR spectra were recorded on a Nexus 670 FT-IR spectrometer (ThermoNicolet) using KBr pellets (400–4000 cm^{-1}) and the Nujol technique (150–600 cm^{-1}). A Raman spectrometer Nicolet NXR 9650 equipped with the liquid nitrogen cooled NXE Genie germanium detector (ThermoNicolet) was used to record Raman spectra of all the complexes (150–4000 cm^{-1}). ¹H and ¹³C NMR spectra of the DMF-*d*₇ solutions were measured on a Varian 400 MHz NMR spectrometer at 300 K. Tetramethylsilane (TMS) was used as an internal reference standard during ¹H and ¹³C NMR experiments. Mass spectra of the methanol solutions of the complexes were obtained by an LCF Fleet ion trap mass spectrometer by the positive mode electrospray ionization (ESI+) technique (Thermo Scientific). The theoretical values were calculated by the QualBrowser software (version 2.0.7, Thermo Fisher Scientific). The electrospray-ionization mass spectrometry interaction experiments were performed on an Agilent HP1100 LC-MSD VL ion-trap mass spectrometer in positive ionization mode. Thermogravimetric (TG) and differential thermal analyses (DTA) were performed using a thermal analyzer Exstar TG/DTA 6200 (Seiko Instruments Inc.) in dynamic air conditions (150

mL min⁻¹) between room temperature (~25 °C) and 900 °C (gradient 2.5 °C min⁻¹).

Synthesis of [Au(L₁)(PPh₃)]·H₂O (1), [Au(L₂)(PPh₃)] (2), [Au(L₃)(PPh₃)] (3), [Au(L₄)(PPh₃)] (4), [Au(L₅)(PPh₃)]·1.5H₂O (5), [Au(L₆)(PPh₃)] (6), [Au(L₇)(PPh₃)] (7), [Au(L₈)(PPh₃)] (8). The amount of 1 mmol of [AuCl(PPh₃)]^{70,71} dissolved in acetone (20 mL) was added to a solution of 1 mmol of the appropriate 6-benzylaminopurine derivative (HL₁–HL₈) in acetone (70 mL). Aqueous 1 M NaOH (1 mL) was added to this mixture. NaCl formed during 4 h of stirring, and it was filtered off. The obtained colorless clear filtrate was evaporated to dryness at 50 °C. The residue was dissolved in 30 mL of benzene. The clear solution was added dropwise into 250 mL of hexane. White precipitates of 1–8 were filtered off, washed with a small amount of ethanol and acetone, and dried at 40 °C under an infrared lamp.

Complex 1: ¹H NMR (400.00 MHz, DMF-*d*₇, ppm): δ (SiMe₄) 8.15 (bs, C2H, 1H), 7.96 (bs, C8H, 1H), 7.77 (m, C2H, C6H, 6H, PPh₃), 7.70 (m, C3H, C4H, C5H, 9H, PPh₃), 7.55 (bs, N6H, 1H), 7.42 (tt, 7.9, 1.6, C14H, 1H), 7.38 (qq, 7.5, 1.6, C15H, 1H), 7.13 (d, 9.2, C12H, 1H), 7.03 (t, 7.5, C13H, 1H), 5.09 (bs, C9H, 2H). ¹³C NMR (75.43 MHz, DMF-*d*₇, ppm): δ (SiMe₄) 162.05, 159.14 (C11), 156.39 (C6), 151.53 (C2), 148.52 (C8), 145.25 (C4), 135.06, 134.92 (C2, C6, PPh₃), 131.09, 130.06 (C14), 130.67, 130.47 (C15), 130.46, 130.34 (C3, C5, PPh₃), 129.21 (C10), 129.82, 129.28 (C1, PPh₃), 129.12, 129.04 (C4, PPh₃), 124.02, 124.00 (C13), 120.96 (C5), 114.64, 114.43 (C12), 39.15 (C9). ESI+ mass spectra (methanol, *m/z*) 244 (calcd 243), 702 (701). Yield: 55%. Anal. Calcd for C₃₀H₂₆N₅OFPAu: C, 50.0; H, 3.6; N, 9.7. Found: C, 50.3; H, 3.8; N, 9.9%.

Complex 3: ¹H NMR (400.00 MHz, DMF-*d*₇, ppm): δ (SiMe₄) 8.13 (s, C2H, 1H), 7.93 (s, C8H, 1H), 7.77 (m, C2H, C6H, 6H, PPh₃), 7.70 (m, C3H, C4H, C5H, 9H, PPh₃), 7.41 (d, 8.5, C12H, C15H, 2H), 7.36 (d, 8.5, C13H, C14H, 2H), 5.14 (bs, C9H, 2H). ¹³C NMR (75.43 MHz, DMF-*d*₇, ppm): δ (SiMe₄) 156.38 (C6), 151.51 (C2), 148.44 (C8), 141.10 (C4), 139.10 (C10), 135.06, 134.92 (C2, C6, PPh₃), 131.11 (C15), 131.07 (C12), 130.47, 130.35 (C3, C5, PPh₃), 129.86 (C14), 129.78, 129.16 (C1, PPh₃), 129.40, 129.27 (C4, PPh₃), 120.92 (C5), 43.86 (C9). ESI+ mass spectra (methanol, *m/z*) 259 (calcd 258), 718 (717), 740 (740). Yield: 60%. Anal. Calcd for C₃₀H₂₄N₅ClPAu: C, 50.1; H, 3.3; N, 9.7. Found: C, 50.0; H, 3.3; N, 9.9%.

Complex 6: ¹H NMR (400.00 MHz, DMF-*d*₇, ppm): δ (SiMe₄) 8.14 (s, C2H, 1H), 7.92 (bs, C8H, 1H), 7.78 (m, C2H, C6H, 6H, PPh₃), 7.70 (m, C3H, C4H, C5H, 9H, PPh₃), 7.50 (bs, N6H, 1H), 7.21 (s, C11H, 1H), 7.20 (m, C15H, 1H), 7.11 (t, 7.5, C14H, 1H), 7.01 (d, 7.5, C13H, 1H), 4.97 (bs, C9H, 2H). ¹³C NMR (75.43 MHz, DMF-*d*₇, ppm): δ (SiMe₄) 154.06 (C6), 151.57 (C2), 148.31 (C8), 145.15 (C4), 139.51 (C10), 139.25 (C12), 135.05, 134.92 (C2, C6, PPh₃), 130.47, 130.35 (C3, C5, PPh₃), 129.38, 129.26 (C4, PPh₃), 128.14 (C14), 128.04 (C13), 128.02 (C11), 125.67 (C15), 121.16 (C5), 44.58 (C9). ESI+ mass spectra (methanol, *m/z*) 239 (calcd 238), 698 (697). Yield: 55%. Anal. Calcd for C₃₁H₂₇N₅PAu: C, 53.3; H, 3.8; N, 10.0. Found: C, 53.6; H, 3.8; N, 10.1%.

The results of NMR, mass spectrometry and elemental analyses (for 2, 4, 5, 7, and 8), IR and Raman spectroscopy, and conductivity measurements (for 1–8) are given in Supporting Information.

Biological Activity Testing. Chemicals and Biochemicals. The RPMI 1640 medium and penicillin–streptomycin mixture were purchased from Lonza (Verviers, Belgium). Phosphate-buffered saline (PBS), fetal bovine serum (FBS), phorbol myristate acetate (PMA), prednisone (98%≤), Auranofin (98%≤), erythrosin B, and *Escherichia coli* 0111:B4 lipopolysaccharide (LPS) were purchased from Sigma-Aldrich (Steinheim, Germany). Cell proliferation reagent WST-1 was obtained from Roche (Mannheim, Germany). A RealTime ready cell lysis kit (Roche, Mannheim, Germany) served for isolation of RNA from cells and Transcriptor Universal cDNA Master (Roche, Mannheim, Germany) was used for reverse transcription of RNA to cDNA. Specific primers and probes (gene expression assays) for polymerase chain reactions (PCRs) were obtained from Applied Biosystems (Foster City, CA, USA). The following assays were chosen

for the quantification of gene expression: Hs00174128_m1 for TNF-α, Hs00961622_m1 for IL-10, Hs01555410_m1 for IL-1β, Hs00893626_m1 for IL-1RA, Hs01590761_g1 for HMGB1, and 4326315E for β-actin, which served as an internal control of gene expression. Quantitative PCR (qPCR) was performed with Fast Start Universal Probe Master (Roche, Mannheim, Germany). Instant ELISA kits (eBioscience, Vienna, Austria) were used to evaluate the production of TNF-α and IL-1β. Cytoscreen kit (BioSource Europe SA, Nivelles, Belgium) was used to detect the IL-1RA cytokine by the enzyme linked immunosorbent assay (ELISA) method. The supported nitrocellulose membrane 0.2 μm (Bio-Rad, Hercules, CA, USA) and albumin bovine fraction V (pH 7) (BSA) (Serva, Heidelberg, Germany) were used for Western blot. Rabbit polyclonal Anti-HMGB1 and goat polyclonal antirabbit IgG (with conjugated peroxidase) antibodies (Sigma-Aldrich, Saint Louis, MO, USA) were applied for immunodetection. Conjugated peroxidase was detected by Opti-4CN substrate kit (Bio-Rad, Hercules, CA, USA).

Maintenance and Preparation of Macrophages. For the measurement of biological activity, we used the human monocytic leukemia cell line THP-1 (ECACC, Salisbury, UK). The cells were cultivated at 37 °C in the RPMI 1640 medium supplemented with 2 mM L-glutamine, 10% FBS, 100 U/mL of penicillin, and 100 μg/mL of streptomycin in a humidified atmosphere containing 5% CO₂. The stabilized cells (3rd–15th passage) were split into microtitration plates to get a concentration of 100000 cells/mL, and the differentiation to macrophages was induced by a phorbol myristate acetate (PMA) as we described previously.⁷²

Cytotoxicity Testing. The THP-1 cells (floating monocytes, 500000 cells/mL) were incubated in 100 μL of the serum-free RPMI 1640 medium and seeded into 96-well plates in triplicate at 37 °C. Measurements were taken 24 h after the treatment with 0.024, 0.12, 0.6, 1.56, 3.13, 6.25, 12.5, 25, or 50 μM tested compounds dissolved in dimethylsulfoxide (DMSO). Viability was measured by WST-1 test according to manufacturer's manual. The amount of created formazan (which correlates to the number of metabolically active cells in the culture) was calculated as a percentage of the control cells, which were treated only with DMSO and was set up as 100%. The results of the WST-1 test were confirmed by the erythrosine-exclusion test, as was described in a previous paper.⁷³ The cytotoxic LD₅₀ concentrations of the tested compounds were determined by the data from the equation generated by the KURV+ Version 4.4b software (Conrad Button Software, Arlington, WA, USA).

Prednisone was used for *in vitro* experiments as a control, while indomethacin was used in *in vivo* studies. This experiment design was chosen because of the fact that indomethacin shows negligible effect on the cytokine expression (it is a typical cyclooxygenase inhibitor).⁷³ On the other hand, steroid drugs, such as prednisone or dexamethasone, are able to affect gene expression.⁷⁴

Drug Treatment and Induction of Inflammatory Response. Differentiated macrophages were pretreated for 1 h with 100 or 600 nM solutions of 1, 3, or 6, 100 nM solution of Auranofin, 1.0 μM solution of prednisone dissolved in DMSO (the final DMSO concentration was 0.1%), and with 0.1% DMSO solution itself (vehicle); the given concentrations of the tested compounds lack the cytotoxic effect (cell viability >94%). The inflammatory response was triggered by adding 1.0 μg/mL lipopolysaccharide (LPS) dissolved in water to pretreated macrophages, control cells were without the LPS treatment. Each experiment was repeated three times.

RNA Isolation and Gene Expression Evaluation. To evaluate the expression of TNF-α, IL-1β, IL-1RA, IL-10, HMGB1, and β-actin mRNA, the total RNA was isolated directly from the cells in cultivation plates using a RealTime ready cell lysis kit according to the manufacturer's instructions. The concentration and purity of the RNA were determined by UV spectrophotometry.

The gene expression was quantified by two-step reverse-transcription quantitative (real-time) PCR (RT-qPCR). The reverse transcription step was performed by Transcriptor Universal cDNA Master using cell lysate as a template. The reaction consists of three steps: (1) primer annealing 29 °C for 10 min and (2) reverse transcription 55 °C for 10 min and (3) transcriptase inactivation 85 °C

for 5 min. A Fast Start Universal Probe Master and gene expression assays were used for qPCR. These assays contain specific primers and TaqMan probes that bind to an exon–exon junction to avoid DNA contamination. The parameters for the qPCR work were adjusted according to the manufacturer's recommendations: 50 °C for 2 min, then 95 °C for 10 min, followed by 40 cycles at 95 °C for 15 s and 60 °C for 1 min. The results were normalized to the amount of ROX reference dye, and the change in gene expression was determined by the $\Delta\Delta C_T$ method.⁷⁵ Transcription of the control cells was set as 1, and other experimental groups were multiples of this value.

Evaluation of Cytokine Secretion by ELISA. Macrophages, which were pretreated with the tested compounds for 1 h, were incubated with LPS for next 24 h. After this period, the medium was collected and the concentration of TNF- α , IL-1 β , and IL-1RA was measured by either Instant ELISA kit or Cytoscreen kit according to the manufactures' manual.

Determination of HMGB1 Release by Western Blot. Media from LPS-stimulated macrophages were obtained similarly as for ELISA. They were lyophilized, and the resting material was resuspended in the 1/10 of the original volume. The same volumes of samples were resolved in the 15% polyacrylamide gel. Then they were electrophoretically transferred on the nitrocellulose membranes, which were subsequently blocked by 5% BSA dissolved in TBST buffer [150 mM NaCl, 10 mM Tris base, 0.1% (v/v) Tween-20]. The membranes were incubated with the primary anti-HMGB1 antibody at the concentration of 1:500 at 4 °C 16 h. After washing, the secondary antirabbit IgG antibody diluted 1:2000 was applied on the membranes and incubated for 1 h at laboratory temperature (~23 °C). The amount of the bound secondary antibody was colorimetrically detected by Opti-4CN kit according to the manufacturer's manual.

Animals. Wistar-SPF (6–8 weeks male) rats were obtained from the AnLab, Ltd., Prague. The animals were kept in plexiglass cages at the constant temperature of 22 ± 1 °C and relative humidity of $55 \pm 5\%$ for at least 1 week before the experiment. They were given food and water ad libitum. All experimental procedures were performed according to the National Institutes of Health (NIH) *Guide for the Care and Use of Laboratory Animals*. In addition, all tests were conducted under the guidelines of the International Association for the Study of Pain.⁷⁶ After a 1-week adaptation period, male Wistar-SPF rats (200–250 g) were randomly assigned to three groups ($n = 10$) of the animals in the study. The control group received 25% DMSO (v/v in water for injections PhEur, intraperitoneal; ip). The other three groups include a carrageenan-treated, an Auranofin positive control (Auranofin + carrageenan), and indomethacin positive control groups (indomethacin + carrageenan).

Carrageenan-Induced Hind Paw Edema. The carrageenan-induced hind paw edema model was used for the determination of anti-inflammatory activity.⁷⁷ Animals were ip pretreated with complexes 1, 3, and 6 (10 mg/kg), Auranofin (10 mg/kg), indomethacin (5 mg/kg), or 25% DMSO (v/v in water for injections PhEur) 30 min prior to the injection of 1% Carr (50 μ L) into the plantar side of right hind paws of the rats. The paw volume was measured immediately after carrageenan injection and during the next 6 h after the administration of the edematogenic agent using a plethysmometer (model 7159, Ugo Basile, Varese, Italy). The degree of swelling induced was evaluated by the percentage of change of the volume of the right hind paw after carrageenan treatment from the volume of the right hind paw before carrageenan treatment. Auranofin and indomethacin were used as positive controls. After 6 h, the animals were sacrificed and the carrageenan-induced edema feet were dissected for cytological and histochemical evaluation.

Histological Examination. For the histological examination, biopsies of paws were taken 6 h following the intraplantar injection of carrageenan. The tissue slices were fixed in 4% buffered formaldehyde for 1 week at room temperature, dehydrated by graded ethanol, and embedded in paraffin (Histowax). The sections (thickness 5 μ m) were deparaffinized with xylene and stained with hematoxylin and eosin (H&E) stain and immunohistochemistry detection apoptosis: caspase 3 (AbCam), TNF- α (AbCam), and CD62E (AbCam). All samples were observed and photographed with

BX-40 Olympus microscopy. Every 3–5 tissue slices were randomly chosen from carrageenan, indomethacin, Auranofin, and studied gold(I) complexes groups. The histological examination of these tissue slices revealed an excessive inflammatory response with massive infiltration of neutrophils [polymorphonuclear leukocytes (PMNs)] by microscopy.

Statistical Analysis. All experiments were performed in three independent experiments, and results are presented as mean values, with error bars representing the standard deviation (SE) of the mean. A one-way ANOVA test was used for statistical analysis, followed by a Tuckey's posthoc test for multiple comparisons. A value of $p < 0.05$ was considered to be statistically significant. GraphPad Prism 5.02 (GraphPad Software Inc., San Diego, CA) was used to perform the analysis.

■ ASSOCIATED CONTENT

📄 Supporting Information

The structural formulas of the 6-benzylaminopurine derivatives HL₁–HL₈, TG/DTA curves of the selected complexes, the figure showing the ESI+ mass spectra of 1 and 3, a geometry of the complex [Au(L₁)(PPh₃)] (1) optimized at the B3LYP/LACVP+** level, a plot showing the effects of 1, 3, 6 (applied at the concentration of 100 nM), Auranofin and vehicle (DMSO) on the LPS-induced TNF- α and IL-1 β secretion, the ESI+ mass spectra of the interactions of 1 and 6 with a mixture of cysteine and glutathione, selected ¹H and ¹³C NMR coordination shifts, the discussion of quantum chemical calculations and selected experimental data (the results of NMR, mass spectrometry and elemental analyses (for 2, 4, 5, 7, and 8), IR and Raman spectroscopy and conductivity measurement (for 1–8)). This material is available free of charge via the Internet at <http://pubs.acs.org>.

■ AUTHOR INFORMATION

Corresponding Author

*Phone: +420 585 634 352. Fax: +420 585 634 954. E-mail: zdenek.travnicek@upol.cz.

Notes

The authors declare no competing financial interest.

■ ACKNOWLEDGMENTS

This research was supported by the Ministry of Education, Youth and Sports of the Czech Republic (grant no. MSM6198959218), the Operational Program Research and Development for Innovations—European Regional Development Fund (CZ.1.05/2.1.00/03.0058), the Operational Program Education for Competitiveness—European Social Fund (CZ.1.07/2.3.00/20.0017) by Palacký University (student project PrF_2011_014 and PrF_2012_009). We thank Dr. Igor Popa for performing NMR experiments, Pavla Richterová for performing CHN elemental analyses, Radka Novotná for IR and Raman spectra measurements, and Alena Klanicová for mass spectra measurements.

■ REFERENCES

- (1) Davies, P. J. *Plant Hormones*; Springer: Dordrecht, 1997.
- (2) Meijer, L.; Borgne, A.; Mulner, O.; Chong, J. P. J.; Blow, J. J.; Inagaki, N.; Inagaki, M.; Delcros, J. G.; Moulinoux, J. P. Biochemical and cellular effects of roscovitine, a potent and selective inhibitor of the cyclin-dependent kinases cdc2, cdk2 and cdk5. *Eur. J. Biochem.* **1997**, *243*, 527–536.
- (3) Benson, C.; Kaye, S.; Workman, P.; Garret, M.; Walton, M.; de Bono, J. Clinical anticancer drug development: targeting the cyclin-dependent kinases. *Br. J. Cancer* **2005**, *92*, 7–12.

- (4) Trávníček, Z.; Matiková-Mal'arová, M.; Novotná, R.; Vančo, J.; Štěpánková, K.; Suchý, P. In vitro and in vivo biological activity screening of Ru(III) complexes involving 6-benzylaminopurine derivatives with higher pro-apoptotic activity than NAMI-A. *J. Inorg. Biochem.* **2011**, *105*, 937–948.
- (5) Trávníček, Z.; Štarha, P.; Popa, I.; Vrzal, R.; Dvořák, Z. Roscovitine-based CDK inhibitors acting as N-donor ligands in the platinum(II) oxalato complexes: preparation, characterization and in vitro cytotoxicity. *Eur. J. Med. Chem.* **2010**, *45*, 4609–4614.
- (6) Vrzal, R.; Štarha, P.; Dvořák, Z.; Trávníček, Z. Evaluation of in vitro cytotoxicity and hepatotoxicity of platinum(II) and palladium(II) oxalato complexes with adenine derivatives as carrier ligands. *J. Inorg. Biochem.* **2010**, *104*, 1130–1132.
- (7) Štarha, P.; Trávníček, Z.; Herchel, R.; Popa, I.; Suchý, P.; Vančo, J. Dinuclear copper(II) complexes containing 6-(benzylamino)purines as bridging ligands: synthesis, characterization, and in vitro and in vivo antioxidant activities. *J. Inorg. Biochem.* **2010**, *103*, 432–440.
- (8) Gielen, M.; Tiekink, E. R. T. *Metallotherapeutic Drugs and Metal-Based Diagnostic Agents*; John Wiley & Sons, Ltd.: New York, 2005.
- (9) Milacic, V.; Ping Dou, Q. The tumor proteasome as a novel target for gold(III) complexes: Implications for breast cancer therapy. *Coord. Chem. Rev.* **2009**, *253*, 1649–1660.
- (10) Ott, I. On the medicinal chemistry of gold complexes as anticancer drugs. *Coord. Chem. Rev.* **2009**, *253*, 1670–1681.
- (11) Nomiyama, K.; Noguchi, R.; Ohsawa, K.; Tsuda, K. Synthesis, crystal structure and antimicrobial activities of two isomeric gold(I) complexes with nitrogen-containing heterocycle and triphenylphosphine ligands, [Au(L)(PPh₃)] (HL = pyrazole and imidazole). *J. Inorg. Biochem.* **2000**, *78*, 363–370.
- (12) Marques, L. L.; Oliveira, G. M.; Lang, E. S. New gold(I) and silver(I) complexes of sulfamethoxazole: synthesis, X-ray structural characterization and microbiological activities of triphenylphosphine-(sulfamethoxazolato-N₂)gold(I) and (sulfamethoxazolato)silver(I). *Inorg. Chem. Commun.* **2007**, *10*, 1083–1087.
- (13) Nomiyama, K.; Yamamoto, S.; Noguchi, R. Ligand-exchangeability of 2-coordinate phosphinegold(I) complexes with AuSP and AuNP cores showing selective antimicrobial activities against Gram-positive bacteria. Crystal structures of [Au(2-Hmpa)(PPh₃)] and [Au(6-Hmna)(PPh₃)] (2-H₂mpa = 2-mercaptpropionic acid, 6-H₂mna = 6-mercaptopyridonic acid). *J. Inorg. Biochem.* **2003**, *95*, 208–220.
- (14) Barreiro, E.; Casas, J. S.; Couce, M. D.; Sánchez, A.; Sánchez-Gonzalez, A.; Sordo, J.; Varela, J. M.; Vázquez López, E. M. Synthesis, structure and cytotoxicity of triphenylphosphinegold(I) sulfanylpropenoates. *J. Inorg. Biochem.* **2008**, *102*, 184–192.
- (15) Lewis, M. G.; DaFonseca, S.; Chomont, N.; Palamara, A. T.; Tardugno, M.; Mai, A.; Collins, M.; Wagner, W. L.; Yalley-Ogunro, J.; Greenhouse, J.; Chirullo, B.; Norelli, S.; Garaci, E.; Savarino, A. Gold drug auranofin restricts the viral reservoir in the monkey AIDS model and induces containment of viral load following ART suspension. *AIDS* **2011**, *25*, 1347–1356.
- (16) Berners-Price, S. J.; Filipovska, A. Gold compounds as therapeutic agents for human diseases. *Metallomics* **2011**, *3*, 863–873 (and the references within).
- (17) Fonteh, P. N.; Keter, F. K.; Meyer, D. HIV therapeutic possibilities of gold compounds. *BioMetals* **2010**, *23*, 185–196.
- (18) Williams, H. J.; Ward, J. R.; Reading, J. C.; Brooks, R. H.; Clegg, D. O.; Skosey, J. L.; Weisman, M. H.; Willkens, R. F.; Singer, J. Z.; Alarcon, G. S.; Field, E. H.; Clements, P. J.; Russell, I. J.; Hochman, R. F.; Boumpas, D. T.; Marble, D. A. Comparison of Auranofin, methotrexate, and the combination of both in the treatment of rheumatoid arthritis. A controlled clinical trial. *Arthritis Rheum.* **1992**, *35*, 259–269.
- (19) Sigler, J. W.; Bluhm, G. B.; Duncan, H.; Sharp, J. T.; Ensign, D. C.; McCrum, W. R. Gold Salts in the Treatment of Rheumatoid Arthritis: A Double-Blind Study. *Ann. Intern. Med.* **1974**, *80*, 21–26.
- (20) Pope, J. E.; Hong, P.; Koehler, B. E. Prescribing trends in disease modifying, antirheumatic drugs for rheumatoid arthritis: a survey of practicing Canadian rheumatologists. *J. Rheumatol.* **2002**, *29*, 255–260.
- (21) Benedek, T. G. The history of gold therapy for tuberculosis. *J. Hist. Med. Allied Sci.* **2004**, *59*, 50–89.
- (22) Kean, W. F.; Kean, I. R. L. Clinical Pharmacology of gold. *Inflammopharmacology* **2008**, *16*, 112–125.
- (23) Kean, W. F.; Hart, L.; Buchanan, W. W. Auranofin. *Br. J. Rheumatol.* **1997**, *36*, 560–572.
- (24) Eisler, R. Chrysotherapy: a synoptic review. *Inflamm. Res.* **2003**, *52*, 487–501.
- (25) Whitehouse, M. W.; Graham, G. G. Is local biotransformation the key to understanding the pharmacological activity of salicylates and gold drugs? *Inflamm. Res.* **1996**, *45*, 579–592.
- (26) Canumalla, A. J.; Al-Zamil, N.; Phillips, M.; Isab, A. A.; Shaw, C. F., III. Redox and ligand exchange reactions of potential gold(I) and gold(III)-cyanide metabolites under biomimetic conditions. *J. Inorg. Biochem.* **2001**, *85*, 67–76.
- (27) Graham, G. G.; Kettle, A. J. The activation of gold complexes by cyanide produced by polymorphonuclear leukocytes. The formation of aurocyanide by myeloperoxidase. *Biochem. Pharmacol.* **1998**, *56*, 307–312.
- (28) Goebel, C.; Kubicka-Muranyi, M.; Tonn, T.; Gonzalez, J.; Gleichmann, E. Phagocytes render chemicals immunogenic: oxidation of gold(I) to the T cell-sensitizing gold(III) metabolite generated by mononuclear phagocytes. *Arch. Toxicol.* **1995**, *69*, 450–459.
- (29) Zou, J.; Guo, Z.; Parkinson, J. A.; Chen, Y.; Sadler, P. J. Gold(III)-induced oxidation of glycine: relevance to the toxic side-effects of gold drugs. *J. Inorg. Biochem.* **1999**, *74*, 352–352.
- (30) Abraham, G. E.; Himmel, P. B. Management of rheumatoid arthritis: rationale for the use of colloidal metallic gold. *J. Nutr. Environ. Med.* **1997**, *7*, 295–305.
- (31) Walz, E. T.; Dimartino, M. J.; Griswold, D. E.; Intoccia, A. P.; Flanagan, T. L. Biologic actions and pharmacokinetic studies of auranofin. *Am. J. Med.* **1983**, *75*, 90–108.
- (32) Kean, W. F.; Kassam, Y. B.; Lock, C. J. L.; Buchanan, W. W.; Rischke, J.; Nablo, L. Antithrombin activity of gold sodium thiomalate. *Clin. Pharmacol. Ther.* **1984**, *35*, 627–632.
- (33) Gunatilleke, S. S.; Barrios, A. M. Inhibition of lysosomal cysteine proteases by a series of Au(I) complexes: a detailed mechanistic investigation. *J. Med. Chem.* **2006**, *49*, 3933–3937.
- (34) Janoff, A. Inhibition of human granulocyte elastase by gold sodium thiomalate. *Biochem. Pharmacol.* **1970**, *19*, 626–628.
- (35) Asperger, S.; Cetina-Cizmek, B. Metal complexes in tumour therapy. *Acta Pharm. (Zagreb, Croatia)* **1999**, *49*, 225–236.
- (36) Brown, D. H.; Smith, W. E. The chemistry of the gold drugs used in the treatment of rheumatoid arthritis. *Chem. Soc. Rev. (London)* **1980**, *9*, 217–240.
- (37) Sato, H.; Yamaguchi, M.; Shibasaki, T.; Ishii, T.; Bannai, S. Induction of stress proteins in mouse peritoneal macrophages by the antirheumatic agents gold sodium thiomalate and auranofin. *Biochem. Pharmacol.* **1995**, *49*, 1453–1457.
- (38) Heimburger, M.; Lerner, R.; Palmblad, J. Effects of antirheumatic drugs on adhesiveness of endothelial cells and neutrophils. *Biochem. Pharmacol.* **1998**, *56*, 1661–1669.
- (39) Rubbiani, R.; Kitanovic, I.; Alborzina, H.; Can, S.; Kitanovic, A.; Onambale, L. A.; Stefanopoulou, M.; Geldmacher, Y.; Sheldrick, W. S.; Wolber, G.; Prokop, A.; Wöfl, S.; Ott, I. Benzimidazol-2-ylidene Gold(I) Complexes Are Thioredoxin Reductase Inhibitors with Multiple Antitumor Properties. *J. Med. Chem.* **2010**, *53*, 8608–8618.
- (40) Yan, K.; Lok, C.-N.; Bierla, K.; Che, C.-M. Gold(I) complex of N,N'-disubstituted cyclic thiourea with in vitro and in vivo anticancer properties—potent tight-binding inhibition of thioredoxin reductase. *Chem. Commun.* **2010**, *46*, 7691–7693.
- (41) Magherini, F.; Modesti, A.; Bini, L.; Puglia, M.; Landini, I.; Nobili, S.; Mini, E.; Cinelli, M. A.; Gabbiani, C.; Messori, L. Exploring the biochemical mechanisms of cytotoxic gold compounds: a proteomic study. *J. Biol. Inorg. Chem.* **2010**, *15*, 573–582.
- (42) Merchant, B. Gold, the noble metal and the paradoxes of its toxicology. *Biologicals* **1998**, *26*, 49–59.
- (43) Gardea-Torresdey, J. L.; Tiemann, K. J.; Gamez, G.; Dokken, K.; Cano-Aguilera, I.; Furenliid, L. R.; Renner, M. W. Reduction and

Accumulation of Gold(III) by *Medicago sativa* Alfalfa Biomass: X-ray Absorption Spectroscopy, pH, and Temperature Dependence. *Environ. Sci. Technol.* **2000**, *34*, 4392–4396.

(44) Abraham, G. E.; Himmel, P. B. Management of rheumatoid arthritis: rationale for the use of colloidal metallic gold. *J. Nutr. Environ. Med.* **1997**, *7*, 295–305.

(45) Rosopulos, Y.; Nagel, U.; Beck, W. Metal complexes with biologically important ligands. 34. Allyl-palladium and triphenylphosphane gold(I) complexes with nucleobases and nucleosides. *Chem. Ber.* **1985**, *118*, 931–942.

(46) Tiekink, E. R. T.; Kurucsev, T.; Hoskins, B.F. J. X-ray structure and UV spectroscopic studies of (adeninato-N9)-triphenylphosphinegold(I). *Crystallogr. Spectrosc. Res.* **1989**, *19*, 823–839.

(47) Becke, A. D. A new mixing of Hartree–Fock and local density functional theories. *J. Chem. Phys.* **1993**, *98*, 1372–1377.

(48) Rassolov, V.; Pople, J. A.; Ratner, M.; Redfern, P. C.; Curtiss, L. A. 6-31G* Basis Set for Third-Row Atoms. *J. Comput. Chem.* **2001**, *22*, 976–984.

(49) Shao, V.; Molnar, L. F.; Jung, Y.; Kussmann, J.; Ochsenfeld, C.; Brown, S. T.; Gilbert, A. T. B.; Slipchenko, L. V.; Levchenko, S. V.; O'Neill, D. P.; DiStasio, R. A., Jr.; Lochan, R. C.; Wang, T.; Beran, G. J. O.; Besley, N. A.; Herbert, J. M.; Lin, C. Y.; Van Voorhis, T.; Chien, S. H.; Sodt, A.; Steele, R. P.; Rassolov, V. A.; Maslen, P. E.; Korambath, P. P.; Adamson, R. D.; Austin, B.; Baker, J.; Byrd, E. F. C.; Dachsel, H.; Doerksen, R. J.; Dreuw, A.; Dunietz, B. D.; Dutoi, A. D.; Furlani, T. R.; Gwaltney, S. R.; Heyden, A.; Hirata, S.; Hsu, C. P.; Kedziora, G.; Khalliulin, R. Z.; Klunzinger, P.; Lee, A. M.; Lee, M. S.; Liang, W. Z.; Lotan, I.; Nair, N.; Peters, B.; Proynov, E. I.; Pieniazek, P. A.; Rhee, Y. M.; Ritchie, J.; Rosta, E.; Sherrill, C. D.; Simmonett, A. C.; Subotnik, J. E.; Woodcock, H. L., III; Zhang, W.; Bell, A. T.; Chakraborty, A. K.; Chipman, D. M.; Keil, F. J.; Warshel, A.; Hehre, W. J.; Schaefer, H. F.; Kong, J.; Krylov, A. I.; Gill, P. M. W.; Head-Gordon, M. Advances in methods and algorithms in a modern quantum chemistry program package. *Phys. Chem. Chem. Phys.* **2006**, *8*, 3172–3191.

(50) Barciszewski, J.; Massino, F.; Clark, B. F. Kinetin—a multiactive molecule. *Int. J. Biol. Macromol.* **2007**, *40*, 182–192.

(51) Han, S.; Kim, K.; Kim, H.; Kwon, J.; Lee, Y. H.; Lee, C. K.; Song, Y.; Lee, S. J.; Ha, N.; Kim, K. Auranofin inhibits overproduction of pro-inflammatory cytokines, cyclooxygenase expression and PGE2 production in macrophages. *Arch. Pharm. Res.* **2008**, *31*, 67–74.

(52) Jeon, K. I.; Jeong, J. Y.; Jue, D. M. Thiol-reactive metal compounds inhibit NF-kappa B activation by blocking I kappa B kinase. *J. Immunol.* **2000**, *164*, S981–S989.

(53) Seitz, M.; Valbracht, J.; Quach, J.; Lotz, M. Gold sodium thiomalate and chloroquine inhibit cytokine production in monocytic THP-1 cells through distinct transcriptional and posttranslational mechanisms. *J. Clin. Immunol.* **2003**, *23*, 477–484.

(54) Arend, W. P. The balance between IL-1 and IL-1Ra in disease. *Cytokine Growth Factor Rev.* **2002**, *13*, 323–340.

(55) Zetterstrom, C. K.; Jiang, W.; Wahamaa, H.; Ostberg, T.; Aveberger, A. C.; Schierbeck, H.; Lotze, M. T.; Andersson, U.; Pisetsky, D. S.; Erlandsson, H. H. Pivotal advance: inhibition of HMGB1 nuclear translocation as a mechanism for the anti-rheumatic effects of gold sodium thiomalate. *J. Leukocyte Biol.* **2008**, *83*, 31–38.

(56) Schierbeck, H.; Wahamaa, H.; Andersson, U.; Harris, H. E. Immunomodulatory drugs regulate HMGB1 release from activated human monocytes. *Mol. Med.* **2010**, *16*, 343–351.

(57) Lin, R. D.; Mao, Y. W.; Leu, S. J.; Huang, C. Y.; Lee, M. H. The Immuno-Regulatory Effects of *Schisandra chinensis* and Its Constituents on Human Monocytic Leukemia Cells. *Molecules* **2011**, *16*, 4836–4849.

(58) Lampa, J.; Klareskog, L.; Ronnelid, J. Effects of gold on cytokine production in vitro; increase of monocyte dependent interleukin 10 production and decrease of interferon-gamma levels. *J. Rheumatol.* **2002**, *29*, 21–28.

(59) Barreiro, E.; Casas, J. S.; Couce, M. D.; Gato, Á.; Sánchez, A.; Sordo, J.; Varela, J. M.; López, E. M. V. Synthesis, structural characterization, and antiinflammatory activity of

triethylphosphinegold(I) sulfanylpropenoates of the type [(AuPEt₃)₂xspa] [H₂xspa = 3-(aryl)-2-sulfanylpropenoic acid]: an (H₂O)₆ cluster in the lattice of the complexes [(AuPEt₃)₂xspa]·3H₂O. *Inorg. Chem.* **2008**, *47*, 6262–6272.

(60) Coppi, G.; Borella, F.; Gatti, M. T.; Comini, A.; Dall'Asta, L. Synthesis, antiinflammatory and antiarthritic properties of a new tiopronine gold derivative. *Boll. Chim. Farm.* **1989**, *128*, 22–24.

(61) Girard, G. R.; Hill, D. T.; Dimartino, M. J. Evaluation of some tetraalkylammonium gold(I) and gold(III) aurate salts for oral antiinflammatory and antiarthritic activity. *Inorg. Chim. Acta* **1989**, *166*, 141–146.

(62) Shaw, C. F., III; Coffey, M. T.; Klingbeil, J.; Mirabelli, C. K. Application of phosphorus-31 NMR chemical shift: gold affinity correlation to hemoglobin–gold binding and the first interprotein gold transfer reaction. *J. Am. Chem. Soc.* **1988**, *110*, 729–734.

(63) Iqbal, M. S.; Saeed, M.; Taqi, S. G. Erythrocyte Membrane Gold Levels After Treatment with Auranofin and Sodium Aurothiomalate. *Biol. Trace Elem. Res.* **2008**, *126*, 56–64.

(64) Isab, A. A.; Ahmad, S. Applications of NMR spectroscopy in understanding the gold biochemistry. *Spectroscopy* **2006**, *20*, 109–123.

(65) Iqbal, M. S.; Taqi, S. G.; Arif, M.; Wasim, M.; Sher, M. In Vitro Distribution of Gold in Serum Proteins after Incubation of Sodium Aurothiomalate and Auranofin with Human Blood and its Pharmacological Significance. *Biol. Trace Elem. Res.* **2009**, *130*, 204–209.

(66) Saccoccia, F.; Angelucci, F.; Boumis, G.; Brunori, M.; Miele, A. E.; Williams, D. L.; Bellelli, A. On the mechanism and rate of gold incorporation into thiol-dependent flavoreductases. *J. Inorg. Biochem.* **2012**, *108*, 105–111.

(67) Lewis, D.; Capell, H. A.; McNeil, C. J.; Iqbal, M. S.; Brown, D. H.; Smith, W. E. Gold levels produced by treatment with auranofin and sodium aurothiomalate. *Ann. Rheum. Dis.* **1983**, *42*, 566–570.

(68) Salemi, G.; Gueli, M. C.; D'Amelio, M.; Saia, V.; Mangiapane, P.; Aridon, P.; Ragonese, P.; Lupo, I. Blood levels of homocysteine, cysteine, glutathione, folic acid, and vitamin B12 in the acute phase of atherothrombotic stroke. *Neurol. Sci.* **2009**, *30*, 361–364.

(69) Kuhnle, J. A.; Fuller, G.; Corse, J.; Mackey, B. E. Anti-senescent activity of natural cytokinins. *Physiol. Plant.* **1977**, *41*, 14–21.

(70) Mann, F. G.; Wells, A. F.; Purdie, D. The constitution of complex metallic salts: Part IV. The constitution of the phosphine and arsine derivatives of silver and aurous halides. The coordination of the coordinated argentous and aurous complex. *J. Chem. Soc.* **1937**, 1828–1836.

(71) Bruce, M. I.; Nicholson, B. K.; Bin Shawkataly, O. Synthesis of gold-containing mixed-metal cluster complexes. *Inorg. Synth.* **1989**, *26*, 324–328.

(72) Hošek, J.; Závalová, V.; Šmejkal, K.; Bartoš, M. Effect of Diplacogon on LPS-Induced Inflammatory Gene Expression in Macrophages. *Folia Biol. (Krakow, Pol.)* **2010**, *56*, 124–130.

(73) Hošek, J.; Bartoš, M.; Chudík, S.; Dall'acqua, S.; Innocenti, G.; Kartal, M.; Kokoška, L.; Kollar, P.; Kutil, Z.; Landa, P.; Marek, R.; Závalová, V.; Žemlička, M.; Šmejkal, K. Natural Compound Cudraflavone B Shows Promising Anti-inflammatory Properties in Vitro. *J. Nat. Prod.* **2011**, *74*, 614–619.

(74) Bahadır, O.; Çitoglu, G. S.; Ozbek, H.; Dall'Acqua, S.; Hošek, J.; Smejkal, K. Hepatoprotective and TNF- α inhibitory activity of *Zosima absinthifolia* extracts and coumarins. *Fitoterapia* **2011**, *82*, 454–459.

(75) Livak, K. J.; Schmittgen, T. D. Analysis of relative gene expression data using real-time quantitative PCR and the 2(T)(–Delta Delta C) method. *Methods* **2001**, *25*, 402–408.

(76) Zimmermann, M. Ethical guidelines for investigations of experimental pain in conscious animals. *Pain* **1983**, *16*, 109–110.

(77) Chang, H. Y.; Sheu, M. J.; Yang, C. H.; Leu, Z. C.; Chang, Y. S.; Peng, W. H.; Huang, S. S.; Huang, G. J. Analgesic effects and the mechanisms of anti-inflammation of hispolon in mice. *Evidence-Based Complementary Altern. Med.* **2011**, *2011*, Article ID 478246 DOI: 10.1093/ecam/nep027.